

# Molecular dynamics of $\beta$ -CD in water/co-solvent mixtures

Kanokthip Srisuk Boonyarattanakalin ·  
Peter Wolschann · Luckhana Lawtrakul

Received: 7 July 2010 / Accepted: 1 December 2010 / Published online: 26 January 2011  
© Springer Science+Business Media B.V. 2011

**Abstract** Molecular dynamics (MD) simulations on  $\beta$ -cyclodextrin ( $\beta$ -CD) in water, ethanol (EtOH), methanol (MeOH) and mixtures of these solvents have been carried out at 300 K over a time period of 15 ns using the AMBER force field. The hydrated X-ray crystallographic structure has four water molecules inside the cavity, defined by a more precise boundary for the  $\beta$ -CD cavity. From the simulations, 2–4 encapsulated water molecules are most probably found. In an ethanol co-solvent system, the  $\beta$ -CD cavity is occupied with one ethanol molecule located in two discrete sites: below and above the O4(n) plane, which is in agreement with experimental results. In all systems, the average values of tilt angles of the obtained structures are higher than the tilt angles of the X-ray structures. The investigations of the alcohol orientations in co-solvent mixtures reveal the hydrophobic environment of the cavity and the hydrophilic atmosphere at both rims of  $\beta$ -CD.

**Keywords** Beta-cyclodextrin · Co-solvent · Molecular dynamics simulations · Methanol · Ethanol

## Introduction

Cyclodextrins (CDs) are cyclic oligosaccharides, composed of  $\alpha$ -1,4-linked D-glucopyranoside units, forming a truncated cone shape. CDs with different numbers of glucose units (6, 7, or 8 glucose units) are found naturally, and they are referred as  $\alpha$ -,  $\beta$ -, and  $\gamma$ -CD, respectively [1, 2]. The orientation of the individual glucose units of CDs shows that the primary hydroxyl groups at the C6 positions outline the narrow rim, while the secondary hydroxyl groups at C2 and C3 positions outline the wider rim of the truncated cone. Consequently, there is no hydroxyl group present within this cavity and the walls of the cavity exhibit mainly a hydrophobic moiety with some potency as hydrogen bond acceptors. CDs possess therefore a lipophilic environment in their cavity and can potentially interact with guest molecules through van der Waals forces and hydrogen bonding. Therefore, CDs are well suited for forming inclusion complexes with a variety of guest molecules in aqueous solutions [1, 3]. This property of CDs leads to various applications of CD inclusion complexes in many fields including pharmaceutical science [4, 5], catalysis [6], separation technology [7–11], agriculture [12], and chromatography [13, 14].

Beta-cyclodextrin ( $\beta$ -CD) has been widely used because of its availability and a cavity size suitable for a wide range of guest molecules [2]. However,  $\beta$ -CD has a relatively low aqueous solubility (1.85 g/100 mL) [5, 15] that limits the applicability of its inclusion complexes. Various methods have been introduced to enhance the solubility, including the addition of urea [16], metal salts [17], ethanol [18], and 2-propanol [19]. Co-solvents are widely used in the formation of cyclodextrin inclusion complexes. Nelson et al. reported that the contributing of short-chain alcohols in the pyrene/cyclodextrin inclusion complexes produces a longer

K. S. Boonyarattanakalin · L. Lawtrakul (✉)  
School of Bio-Chemical Engineering and Technology,  
Sirindhorn International Institute of Technology, Thammasat  
University, P.O. Box 22, Thammasat Rangsit Post Office,  
Bangkok 12121, Pathum Thani, Thailand  
e-mail: luckhana@siit.tu.ac.th

P. Wolschann  
Institute of Theoretical Chemistry, University of Vienna,  
Währinger Strasse 17, 1090 Vienna, Austria  
e-mail: karl.peter.wolschann@univie.ac.at

lifetime of the pyrene complex than free pyrene [20]. Taghvaei et al. has reported the effects of several common solvents (methanol, dimethylformamide, dimethyl sulfoxide, acetonitrile) on the solubility of  $\beta$ -CD [21]. Chatjigakis et al. has studied the solubility of  $\beta$ -CD in a series of water/co-solvent mixtures for compositions between 0 and 100% mole fraction of the co-solvent [22].

Computational modelling studies on CDs have been performed for a better understanding of the behaviour of CDs at the molecular level. Molecular dynamics (MD) simulations are appropriate to investigate the dynamics of molecular systems using more realistic boundary conditions that could not be acquired by quantum mechanics calculations. Many research groups have been using MD as a main tool for investigating  $\beta$ -CD in aqueous solution [23–26]. However, no systematic simulation study of  $\beta$ -CD in co-solvent systems exists. In this study, MD simulations of  $\beta$ -CD in water/co-solvent mixtures have been carried out. We focused on the  $\beta$ -CD structures and the interactions between  $\beta$ -CD and solvent molecules. Particularly, the number of solvent molecules inside the cavity, where the guest molecule in an inclusion complex resides, was investigated.

## Methodology

The initial molecular geometry of  $\beta$ -CD was obtained from the Cambridge Crystallographic Database (BCDEXD10) [27]. Hydrogen atoms were added to  $\beta$ -CD, then optimized at the HF/6-31G(d,p) level, using Gaussian 03 [28]. The partial atomic charges for  $\beta$ -CD were derived using the restrained electrostatic potential, RESP [29, 30] charge-fitting procedure. The ab initio electrostatic potential for RESP was calculated using the Gaussian 03 program at the HF/6-31G(d) level of theory. Preparation of  $\beta$ -CD force field parameters was done by using the Antechamber module [31] of the AMBER program package.

The MD simulations were performed using the AMBER10 program [32]. The AMBER 2003 force field [33] parameter sets were used for  $\beta$ -CD and all solvent molecules. The LEaP, SANDER, and Ptraj modules were used for preparing the input data, minimizing and MD simulating, and for analyzing the MD trajectories, respectively.

In  $\beta$ -CD/water system,  $\beta$ -CD was immersed in a truncated octahedron box of TIP3P [34] water molecules with a closeness parameter of 10 Å away from the boundary of any  $\beta$ -CD atoms. A total of 1037 water molecules were automatically generated in this box. For  $\beta$ -CD in either water/methanol- or water/ethanol-co-solvent systems, all concentrations of the solutions are calculated in vol/vol

**Table 1** Number of solvent molecules used in the simulations

System	No. of water molecules	No. of alcohol molecules
1% MeOH	3,309	15
50% MeOH	1,670	743
Pure MeOH	–	427
1% EtOH	3,307	10
50% EtOH	1,670	515
Pure EtOH	–	426

The concentrations are given in % (vol/vol)

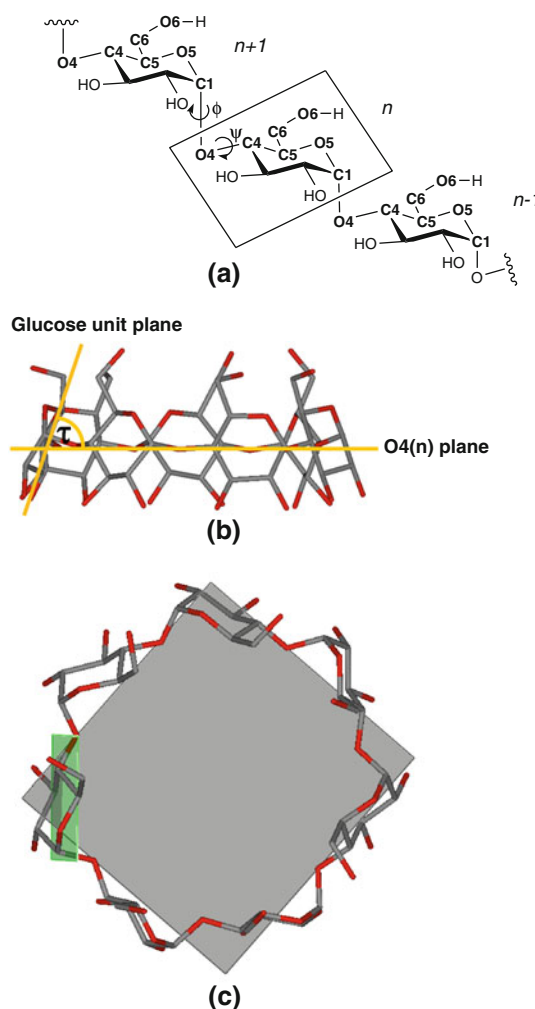


**Fig. 1** **a** Schematic representation of CD fragment showing atomic numbering and torsional angles around glycosidic bonds ( $\phi$  and  $\psi$  defined as  $O5(n)-C1(n)-O4(n-1)-C4(n-1)$  and  $C1(n)-O4(n-1)-C4(n-1)-C5(n-1)$ , respectively), **b** and **c** side and top view representations of tilt angle,  $\tau$  defined as the angle between the  $O4(n)$  mean plane and each least-squares best-fit glucose unit mean plane through  $C1(n)-O5(n)-C5(n)-C4(n)-O4(n)-C3(n)-C2(n)-O4(n-1)$  of  $\beta$ -CD

**Table 2** Selected geometrical parameters of  $\beta$ -CD in water

	Solution		Solid <sup>a</sup>		Gas <sup>b</sup>
	Mean	$\sigma$	Mean	$\sigma$	
Distance (Å)					
O4(n)···O4(n – 1)	4.368	0.187	4.364	0.117	4.431
O4(n)···O4(n – 2)	7.851	0.504	7.854	0.246	7.984
O4(n)···O4(n – 3)	9.465	0.841	9.785	0.327	9.956
O2(n)···O3(n – 1)	3.171	0.704	2.857	0.066	2.852
d	0.178 <sup>c</sup>	0.604	0.165 <sup>c</sup>	0.193	0
Angle (°)					
O4(n + 1)···O4(n)···O4(n – 1)	124.0	10.479	128.3	3.688	128.6
$\tau$	87.0	26.676	77.8	9.946	79.6
Torsion angle (°)					
$\phi$	120.2	31.486	109.9	6.287	114.7
$\psi$	–122.4	29.308	–112.2	8.903	–112.8
O5(n)–C5(n)–C6(n)–O6(n)	–66.3	10.734	–64.4	4.212	–59.3
	65.8	14.717	68.7	3.528	–

d: deviation of O4(n) from the least-squares plane defined by the seven O4(n) atoms;  $\tau$ : tilt angle, defined as the angle between the O4(n) plane and the glucose unit planes;  $\phi$  and  $\psi$ : torsional angles around the glycosidic bonds defined as O5(n)–C1(n)–O4(n – 1)–C4(n – 1) and C1(n)–O4(n – 1)–C4(n – 1)–C5(n – 1), respectively;  $\sigma$ : standard deviation of each parameter

<sup>a</sup> Selected geometrical parameter of the X-ray crystallographic structure [27]

<sup>b</sup> Selected geometrical parameter of the C7 symmetry structure of  $\beta$ -CD from calculations [36]

<sup>c</sup> Is the absolute value of the deviation of O4(n) from the O4(n) mean plane

percents. The details of number of water and alcohol molecules in all co-solvent systems are presented in Table 1.

In all cases, the non-bonded cut-off distance was set to 10.0 Å. The integration time step was 2 fs and the SHAKE algorithm [35] was applied to constrain the bonds involving hydrogen atoms. After initial minimization of the solvent molecules using 5,500 steps of the steepest descent and then conjugate gradient algorithms, the whole system of  $\beta$ -CD and solvent was equilibrated, using the Canonical Ensemble (NVT) for 200 ps with the temperature raised from 0 to 300 K. After that, the Isobaric-Isothermal ensemble (NPT) was performed for 1 ns at 300 K and 1 atm to achieve equilibrium. The simulation was run for 15 ns at 300 K using periodic boundary conditions in the NPT ensemble. The system coordinates was taken every 1 ps during the last 15 ns of the production period. The structural variation information during the simulations was obtained from the root mean square deviation (RMSD).

## Results and discussions

### $\beta$ -CD in aqueous solution

The average root mean square deviation (RMSD) of the MD simulated atomic position from the corresponding

initial atomic positions of  $\beta$ -CD, after equilibration for 15 ns is about 1.19 Å. Figure 2a shows the RMS fluctuation of  $\beta$ -CD in aqueous solution from the initial structure that was obtained from the X-ray Crystallographic structure [27]. For each MD simulation, the RMSD values were calculated for the position of all backbone atoms of  $\beta$ -CD, C1(n)–C2(n)–C3(n)–C4(n)–C5(n)–O4(n)–O5(n) (see also Fig. 1a). The Plot confirms the dynamics of  $\beta$ -CD structure during the simulation time.

Deviations of all structural parameters of  $\beta$ -CD obtained from the simulations from the X-ray structure are significant (Table 2). These differences emphasize the necessity of understanding the dynamic nature of  $\beta$ -CD in aqueous solution in addition to the static nature of the  $\beta$ -CD structure reported in the form of solid phase crystal. The absolute value of the average torsional angles around glycosidic bonds,  $\phi$  and  $\psi$  in solution are higher than the torsional angles of  $\beta$ -CD in solid and gas phase taken from the X-ray crystallographic data [27] and quantum chemistry studies [36]. The  $\beta$ -CD structure in solution is less symmetrical compared with the hydrated  $\beta$ -CD in solid state from the crystal structure. The bending of the  $\beta$ -CD structure is caused by the replacement of the intramolecular hydrogen bond interactions, between the hydroxyl group at C2 and the adjacent hydroxyl group at C3 positions, by intermolecular hydrogen bonds with water molecules. At times, the water molecules act as a hydrogen bond bridge

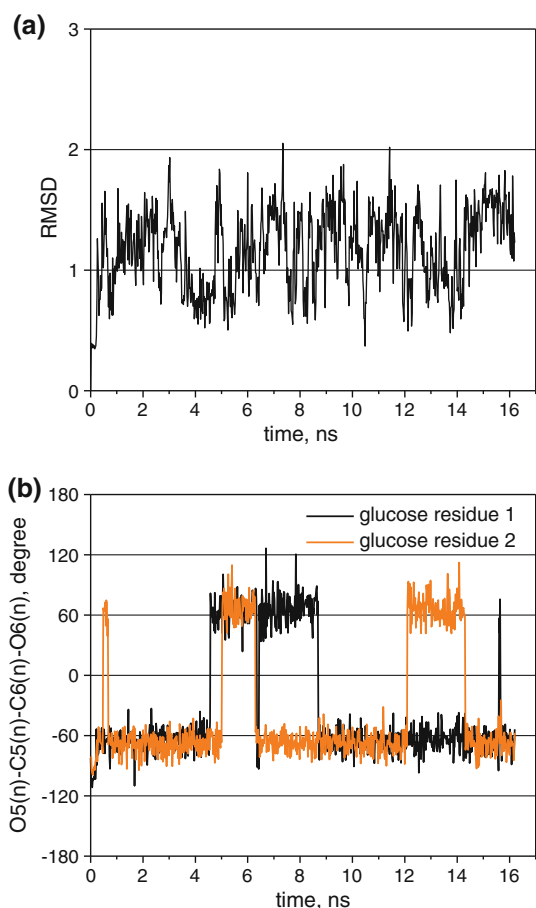


**Fig. 2** **a** Plot of RMSD of  $\beta$ -CD in water, compared with the initial structure as a function of time, for all backbone atoms of  $\beta$ -CD. **b** The orientation of the primary hydroxyl groups relative to the glucose ring, defined as  $O5(n)-C5(n)-C6(n)-O6(n)$  during the MD simulations of  $\beta$ -CD in water

between both adjacent hydroxyl groups. The flip-flop hydrogen bonds can be detected during simulation time and this is in agreement with experimental studies [37]. The disruption by surrounding water molecules on the intramolecular hydrogen bonds, by forming new intermolecular hydrogen bonds with  $\beta$ -CD hydroxyl groups were also reported from Raffaini in 2007 [26]. They showed the loss of symmetry of  $\beta$ -CD in water compared to the isolated  $\beta$ -CD molecule.

Moreover, the interaction of  $\beta$ -CD with water molecules causes the primary hydroxyl groups at the narrow rim to move away from the initial structure. During the simulations, all primary hydroxyl groups are in both (–) and (+) gauche orientations, with respect to O5. The probabilities are 67% for negative and 33% for positive orientations. The orientations of two representative primary hydroxyl groups of  $\beta$ -CD in water are shown in Fig. 2b. The plot shows that the primary hydroxyl groups at C6 positions both point outward and inward from the cavity to form

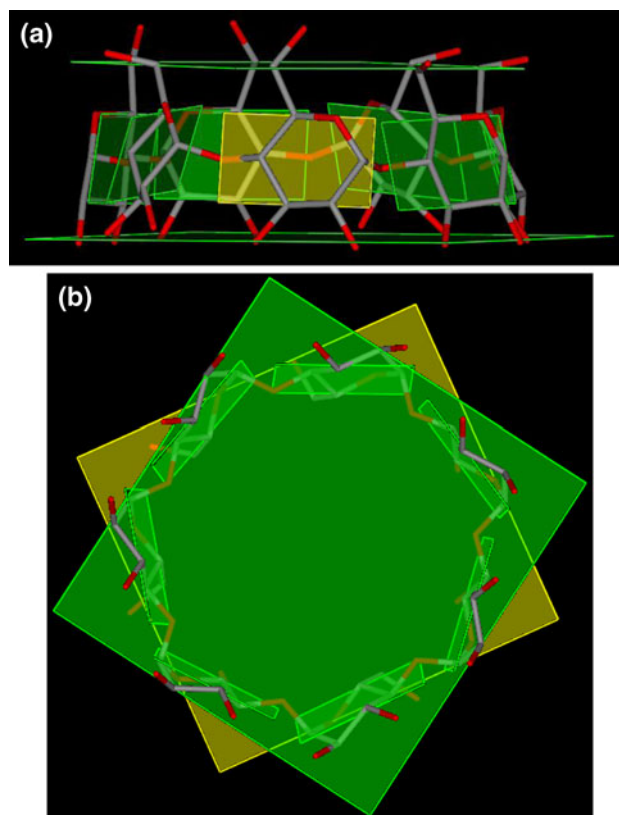


**Fig. 3** Schematic representation of the inner and outer  $\beta$ -CD cavity: *upper* and *lower* planes are defined as the least square plane of  $C6(n)$  and  $O2(n),O3(n)$  atoms. The wall of the cavity, defined as all seven glucose unit planes **a** side view and **b** top view

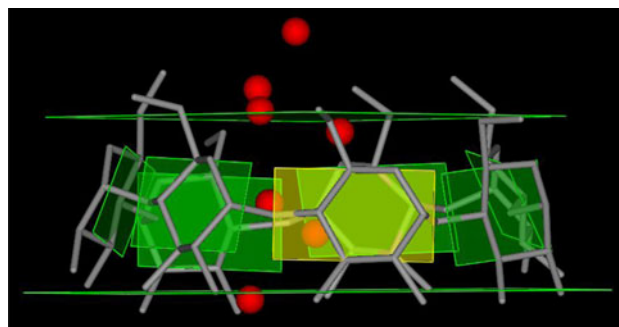


**Fig. 4** Using new criteria to count water molecules inside the cavity of hydrated  $\beta$ -CD in the solid state from the X-ray crystallographic structure [27]: four water molecules are found inside the  $\beta$ -CD cavity

hydrogen bonds with water molecules. In contrast to the X-ray crystallized structure in solid state [27], only one of seven primary hydroxyl groups is disordered over these two orientations. The other four primary hydroxyl groups are in the favoured (–) gauche orientation, while the other two primary hydroxyl groups are in the (+) gauche orientation. The flexibility of the primary hydroxyl group orientation results in a more distorted structure.

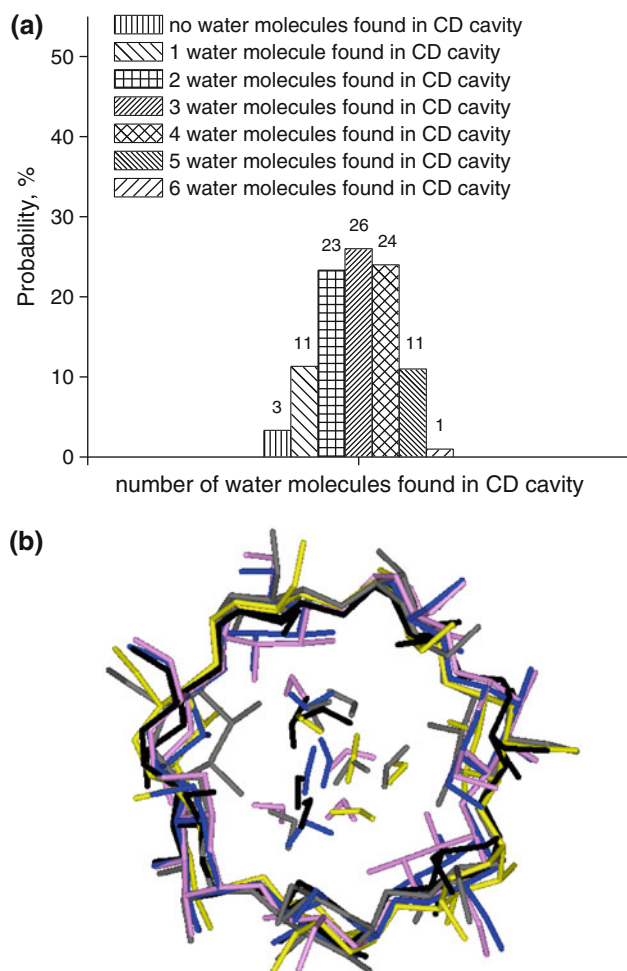


**Fig. 5** **a** Probability distributions of the number of water molecules presented inside the  $\beta$ -CD cavity during the MD simulations for 15 ns of  $\beta$ -CD in water. **b** Superimposition of the snapshot structures of  $\beta$ -CD in water from MD simulations. The black structure represents the X-ray crystal structure [27]. The hydrogen atoms of  $\beta$ -CD are omitted

The shape of  $\beta$ -CD can also be investigated from the value of the tilt angle,  $\tau$  (shown in Fig. 1b and c). If  $\tau = 90^\circ$ , it indicates a perfect cylindrical shape and if  $\tau < 90^\circ$ , it implies conical shape. The simulated structures have an average  $\tau$  angle of about  $10^\circ$  more than the tilt angle found in the X-ray structure. This results in a more steep structure.

In order to understand the dynamic nature of CD in solutions, it is critical to monitor the number of entrapped solvent molecules within the CD cavity. However, the definition of locations inside or outside of the CD cavity is not clear. Because the cavity is not a closed space, it allows a continuous exchange of solvent molecules with the bulk solvent at room temperature. The interaction of CD with solvent molecules causes the distortion of CD as shown above. Consequently, narrow and wider rims do not become co-planar. Raffaini [26] used MD simulations to

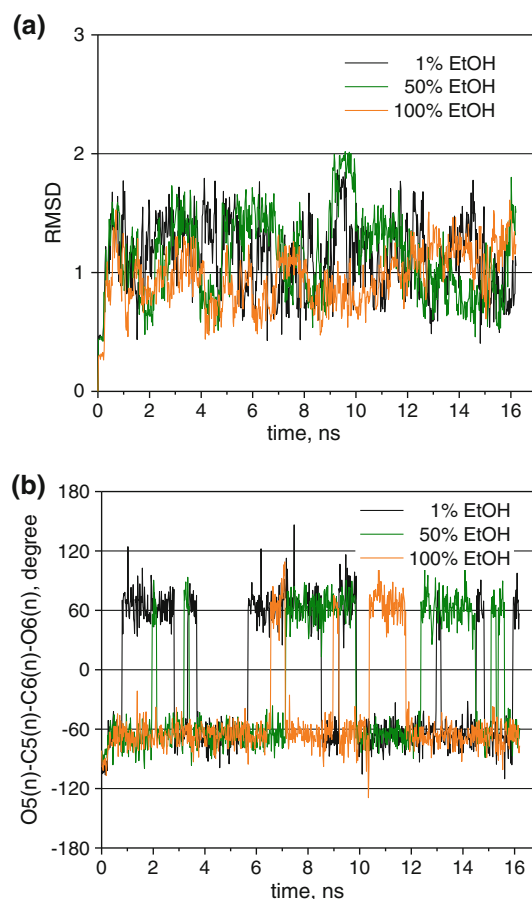


**Fig. 6** **a** Plot of RMSD of  $\beta$ -CD in solution of EtOH from the initial structure as a function of MD simulation time for all backbone atoms of  $\beta$ -CD. **b** The orientation of one primary hydroxyl group relative to the glucose ring, defined as  $O5(n)-C5(n)-C6(n)-O6(n)$  during the MD simulations of  $\beta$ -CD in EtOH

study CDs in water. They calculated the pair distribution function of water molecules around the center of mass of CDs. Water molecules located at a distance from the center of mass, which is less than the average distance of the nearest hydroxyls on both rims, are considered to be inside the cavity. The molecules inside cavity is usually defined by the radius from the center of mass of CD. Solvent molecules that stay within the sphere limited by the radius are considered to be inside the CD cavity. Because of the unsymmetrical nature and conical shape of CD in aqueous solution, some solvent molecules that are actually located outside the CD cavity are considered to be inside the cavity. Therefore, the numbers of solvent molecules inside the CD cavity, measured by the mentioned method, are over-estimated. In addition, the CD boundary during the simulation times is distorted and varied. A more precise definition of space within the CD cavity is necessary.

In this study, in order to monitor the number of solvent molecules that are only located within the dynamic  $\beta$ -CD cavity, a more flexible conical space of  $\beta$ -CD cavity is

**Table 3** Selected geometrical parameters of  $\beta$ -CD in ethanol systems

	Solution						X-ray <sup>a</sup>	
	1% EtOH		50% EtOH		100% EtOH		Mean	$\sigma$
	Mean	$\sigma$	Mean	$\sigma$	Mean	$\sigma$		
Distance (Å)								
O4(n)⋯O4(n – 1)	4.374	0.178	4.382	0.167	4.397	0.155	4.403	0.041
O4(n)⋯O4(n – 2)	7.723	0.443	7.749	0.416	7.816	0.334	7.934	0.071
O4(n)⋯O4(n – 3)	9.527	0.715	9.559	0.640	9.673	0.513	9.892	0.111
O2(n)⋯O3(n – 1)	3.058	0.583	2.980	0.499	2.918	0.365	2.837	0.037
d	0.105 <sup>b</sup>	0.600	0.252 <sup>b</sup>	0.541	0.041 <sup>b</sup>	0.508	0.032 <sup>b</sup>	0.038
Angle (°)								
O4(n + 1)⋯O4(n)⋯O4(n – 1)	124.5	8.904	124.8	8.177	125.7	6.432	128.5	1.379
$\tau$	87.0	25.326	87.9	22.967	86.0	22.357	80.9	3.145
Torsion angle (°)								
$\phi$	122.2	27.579	123.4	24.056	122.5	22.734	112.3	2.829
$\psi_1$	–123.0	22.482	–123.5	21.057	–123.1	20.339	–112.6	2.758
$\psi_2$	115.5	30.007	115.0	26.904	115.7	22.306	127.2	2.644
O5(n)–C5(n)–C6(n)–O6(n)	–66.0	10.864	–65.4	10.868	–65.6	12.263	–64.2	4.990
	66.3	15.181	67.3	15.993	67.0	15.933	49.8	18.223

d: deviation of O4(n) from the least-squares plane defined by the seven O4(n) atoms;  $\tau$ : tilt angle, defined as the angle between the O4(n) plane and the glucose unit planes;  $\phi$ ,  $\psi_1$  and  $\psi_2$ : torsion angles around the glycosidic bonds defined as O5(n)–C1(n)–O4(n – 1)–C4(n – 1), C1(n)–O4(n – 1)–C4(n – 1)–C5(n – 1) and C1(n)–O4(n – 1)–C4(n – 1)–C3(n – 1), respectively;  $\sigma$ : standard deviation of each parameter

<sup>a</sup> Selected geometrical parameter of the X-ray crystallographic structure [40]

<sup>b</sup> Is the absolute value of the deviation of O4(n) from the O4(n) mean plane

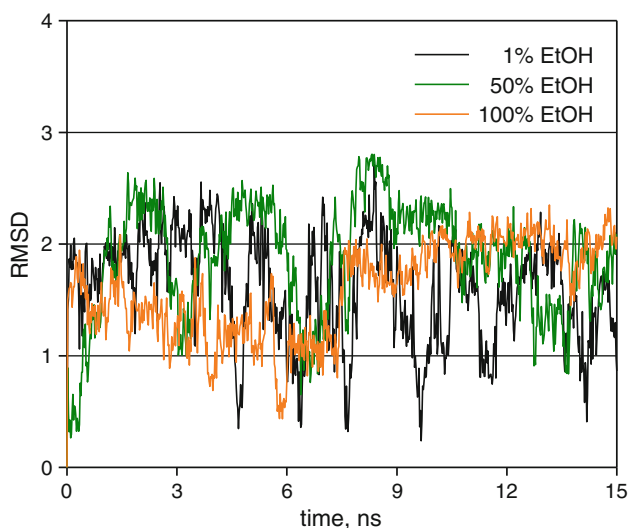


**Fig. 7** Plot of RMSD of  $\beta$ -CD in system of EtOH from the equilibrated structure of  $\beta$ -CD in water as a function of MD simulation time for all backbone atoms

defined to discriminate between the inner and outer cavity of  $\beta$ -CD. The conical shape of the  $\beta$ -CD cavity is composed of planes from each glucose unit present in the individual CD conformation. This reflects the variations in shape and size of  $\beta$ -CD in the solution phase. All the

solvent molecules defined by this boundary to be within the  $\beta$ -CD cavity are actually entrapped inside the cavity.

The space inside the cavity, is defined as the volume that is confined by nine mean planes, including upper and lower planes, and seven mean planes of each glucose unit as shown in Fig. 3. Upper and lower planes are defined as the least square plane of C6(n) and O2(n)–O3(n), respectively. Each glucose unit plane is a common plane of O4(n – 1)–C1(n)–C2(n)–C3(n)–C4(n)–O4(n)–C5(n)–O5(n) atoms. All seven glucose unit planes make up the wall of the cavity. Only molecules in the same direction as the direction of all normal vectors of each plane that point into the cavity, are counted as encapsulated molecules.

The X-ray spectroscopy study [27] reported that the hydrated form of  $\beta$ -CD crystallizing from water contains approximately 6.5 water molecules, distributing over 8 sites within the cavity. In the defined boundary mentioned above, the number of water molecules inside the cavity of crystallographic  $\beta$ -CD is monitored. There are only four water molecules inside the cavity as presented in Fig. 4. While the number of water molecules inside  $\beta$ -CD cavity of the crystal neutron diffraction studies [38, 39] are two and three, based on the newly defined cavity.

In our simulations, all 300 CD structures were analyzed every 50 ps during the last 15 ns after equilibration for counting the encapsulated solvent molecules. The highest

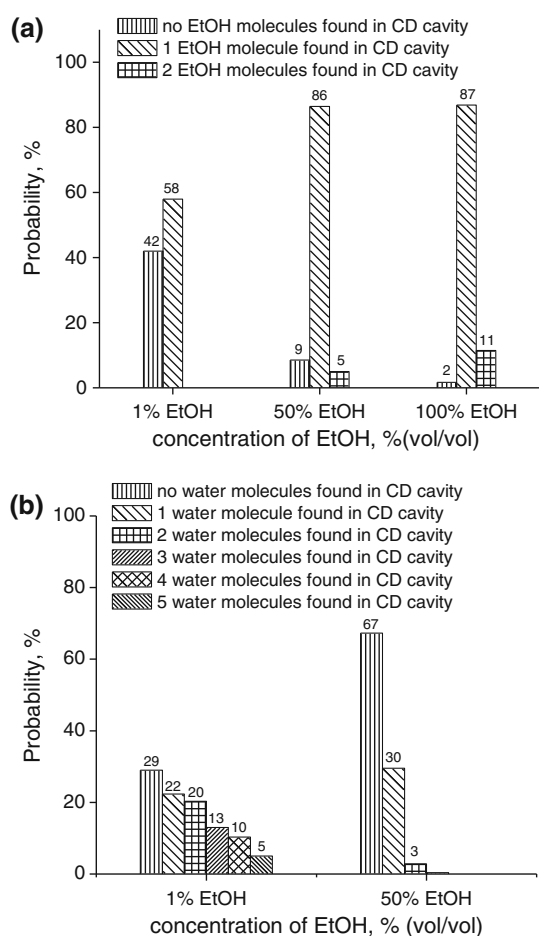


**Fig. 8** Probability distributions of the number of **a** EtOH molecules and **b** water molecules inside the  $\beta$ -CD cavity during the MD simulations for 15 ns of  $\beta$ -CD in an EtOH system

probability of the number of trapped water molecules shows about 2–4 molecules localized in  $\beta$ -CD cavity, as shown in Fig. 5a. The number of encapsulated water molecules obtained from the MD simulations agrees with these experimental data [27, 38, 39].

The superimposition of the snapshot structure of  $\beta$ -CD in water from MD simulations with the X-ray crystal structure [27] is shown in Fig. 5b. The X-ray structure is similar to the snapshots that are obtained from the simulations (see also Table 2). The orientation of the primary hydroxyl group is rather flexible in order to interact with water molecules. The result demonstrates that AMBER 2003 force field can be used to investigate the dynamics of  $\beta$ -CD in solvent systems.

#### $\beta$ -CD in water/ethanol-co-solvent

The average root mean square deviations (RMSD) of the MD simulated atomic position from the corresponding initial atomic positions of  $\beta$ -CD, after equilibration for

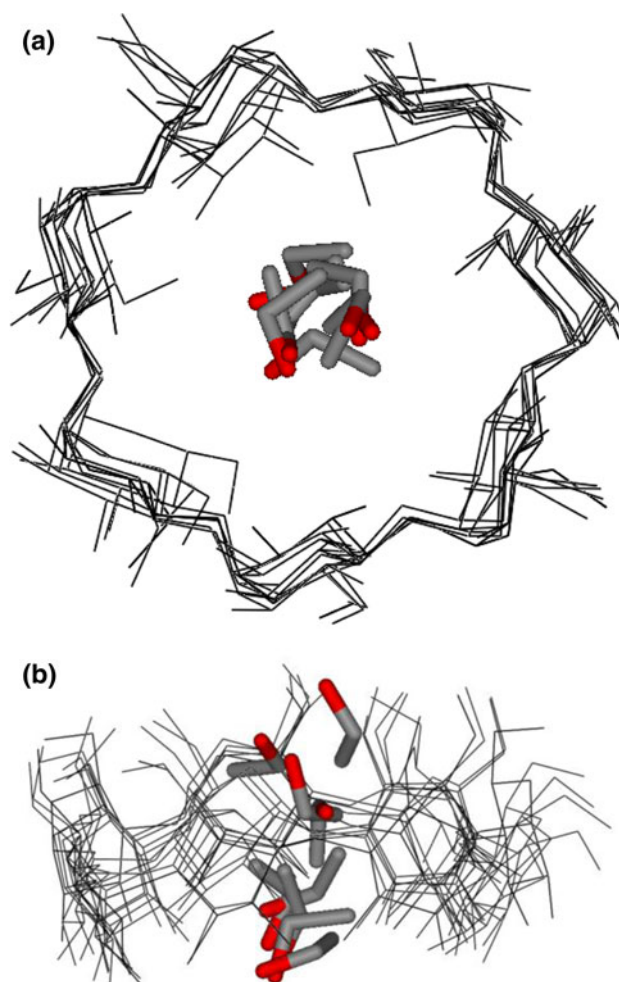


**Fig. 9** Superimposition of the snapshots of an ethanol molecule in  $\beta$ -CD cavity from 8.2 to 8.7 ns of the MD simulations of  $\beta$ -CD in 50% EtOH. The hydrogen atoms are omitted

15 ns, are about 1.13, 1.15 and 0.97 Å for  $\beta$ -CD in 1, 50 and 100% EtOH (Fig. 6a). RMSD values of  $\beta$ -CD molecules are smaller for higher ethanol concentration than dilute concentration.

When the structural parameters of  $\beta$ -CD in different concentrations of ethanol are compared, we found that the change of all values is not significant. However, the standard deviation depends on the amount of ethanol molecules in the system. The standard deviation decreases when the EtOH concentration increases (see Table 3). The results show that the fluctuation of  $\beta$ -CD structure in dilute EtOH solution is higher than that of  $\beta$ -CD in higher EtOH concentration solutions.

The orientations of the primary hydroxyl group (O5(n)–C5(n)–C6(n)–O6(n) torsion angles) in crystal structure at room temperature [40] are usually in both (–) and (+) gauche. Five C6(n)–O6(n) groups show disorder (–)/(+) gauche and two groups are oriented only (–) gauche. For the structure obtained from the simulations, all seven

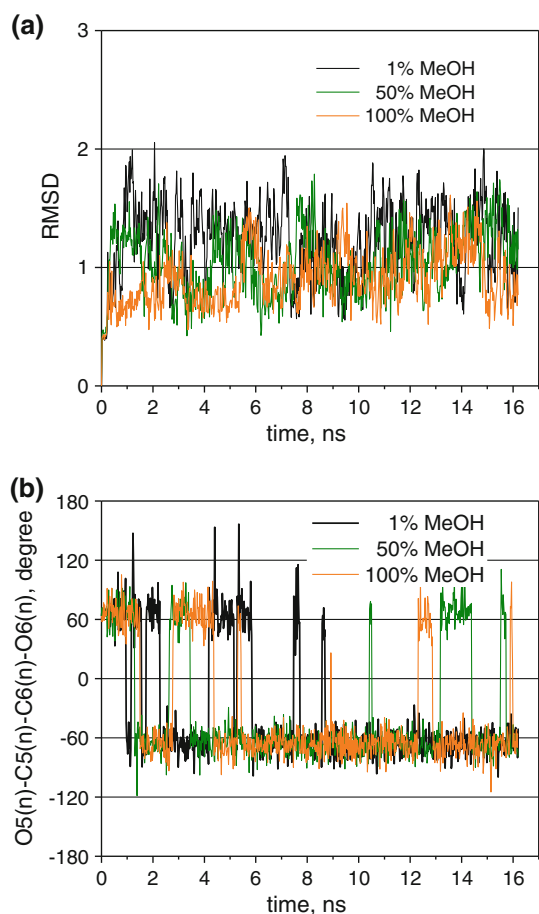


**Fig. 10** **a** Plot of RMSD of  $\beta$ -CD in solution of MeOH from the initial structure as a function of MD simulation time for all backbone atoms of  $\beta$ -CD. **b** The fluctuations of the orientation of the primary hydroxyl groups relative to the glucose ring, defined as  $O5(n)-C5(n)-C6(n)-O6(n)$  during the MD simulations for  $\beta$ -CD in system of MeOH

$C6(n)-O6(n)$  groups are in both (–) and (+) gauche orientations. However, the (–) orientation is more often observed with 64, 72 and 71% probability for  $\beta$ -CD in 1, 50 and 100% concentrations of EtOH, respectively (see also Fig. 6b).

The average tilt angle of  $\beta$ -CD in EtOH systems is about 86–88°, that is approximately 8° more than the X-ray crystal structure [40]. The results show the same trend where the simulations give higher tilt angles than are obtained by X-ray in both aqueous and EtOH co-solvent systems.

In order to investigate the change of  $\beta$ -CD structure in the presence of EtOH, we compared the obtained structure with the previous  $\beta$ -CD structure in 100% water. RMSD from the equilibrated structure of  $\beta$ -CD in water are about 1.16, 1.19 and 1.59 Å for  $\beta$ -CD in 1, 50 and 100% EtOH, respectively (Fig. 7). The standard deviation  $\sigma$ , of all selected geometrical parameters of  $\beta$ -CD in the presence of

ethanol are less than the geometrical parameters of  $\beta$ -CD in aqueous solution. This shows that  $\beta$ -CD in an ethanol system is more rigid than  $\beta$ -CD in water. The rigidity is probably caused by the strain from the interaction between  $\beta$ -CD and the guest molecule (EtOH) inside the cavity.

The  $\beta$ -CD cavity is occupied with one molecule of ethanol (58, 86 and 86% probability for 1, 50 and 100% EtOH, respectively) that show similarity with the experiments [40, 41]. The number of encapsulated solvent molecules is reported in Fig. 8.

For 1% concentration, the site most frequently occupied by EtOH molecule is in the lower part (below  $O4(n)$  plane) of the  $\beta$ -CD cavity (occupancy 0.9) which is in agreement with the X-ray crystallographic structure [41]. This EtOH molecule that is inside the cavity always turns its hydroxyl group to interact with water molecules outside the cavity. The ethyl moiety of the ethanol molecule is inside the cavity. The investigation of the pathway of an ethanol molecule shows that an ethanol molecule always enter the  $\beta$ -CD cavity through the  $C2/C3$  rim. Then it stays inside the cavity for about 2.2 ns and passes through the  $C6$  rim. In this system, the primary hydroxyl groups are found in (+) gauche orientation (37%) more often than in aqueous solution (33%). This  $C6(n)-O6(n)$  orientation stabilizes the EtOH inside the cavity.

For 50% concentration, an encapsulated ethanol molecule always turns its ethyl residue into the cavity and points the hydroxyl outward to form hydrogen bonds with either water molecules or hydroxyl groups of  $\beta$ -CD at both rims. The orientation of ethanol molecules is caused by the hydrophobic property inside the  $\beta$ -CD cavity and the hydrophilic property at the rims of  $\beta$ -CD. The course of ethanol movement in this system shows two frequently occupied sites inside the  $\beta$ -CD cavity as shown in Fig. 9. The occupancy factor for an EtOH molecule at the upper part (above  $O4(n)$  plane) of  $\beta$ -CD cavity is about 0.6. The obtained results are also in agreement with the experimental report from a single crystal neutron diffraction study of partially deuterated  $\beta$ -CD ethanol octahydrate at 295 K, that ethanol molecules are in two different sites in the cavity [41]. The X-ray crystallographic structure study by Steiner group at room temperature reported that an EtOH molecule is located in the lower part of the  $O4(n)$  plane [41], while the other site in the upper part of the  $\beta$ -CD cavity was reported by Aree [40]. This shows that the arrangement of solvent molecules can be different in different crystals. The molecular dynamics study of this system shows both frequently occupied sites inside the  $\beta$ -CD cavity. Intramolecular hydrogen bonds are obviously found during the simulations, and the flip-flop hydrogen bonds of these adjacent hydroxyl groups were detected. Ethanol molecules enter the  $\beta$ -CD cavity through the  $C6$  rim. The molecules stay inside the cavity for 500 ps, then



**Table 4** Selected geometrical parameters of  $\beta$ -CD in methanol systems

Distance ( $\text{\AA}$ )	Solution						X-ray <sup>a</sup>	
	1% MeOH		50% MeOH		100% MeOH		Mean	$\sigma$
	Mean	$\sigma$	Mean	$\sigma$	Mean	$\sigma$		
O4(n)⋯O4(n – 1)	4.353	0.191	4.385	0.170	4.405	0.159	4.379	0.121
O4(n)⋯O4(n – 2)	7.648	0.516	7.771	0.413	7.841	0.347	7.881	0.253
O4(n)⋯O4(n – 3)	9.416	0.865	9.600	0.648	9.716	0.516	9.819	0.337
O2(n)⋯O3(n – 1)	3.213	0.719	2.988	0.529	2.880	0.336	2.866	0.072
d	0.115 <sup>b</sup>	0.620	0.204 <sup>b</sup>	0.516	0.131 <sup>b</sup>	0.461	0.164 <sup>b</sup>	0.074
Angle ( $^\circ$ )								
O4(n + 1)⋯O4(n)⋯O4(n – 1)	123.7	10.766	125.2	8.127	126.1	6.646	128.3	3.772
$\tau$	86.3	27.555	87.8	22.961	88.2	20.990	77.7	11.584
Torsion angle ( $^\circ$ )								
$\phi$	119.7	32.223	123.2	24.717	124.7	20.932	114.0	8.964
$\psi$	–122.0	28.153	–123.5	21.655	–124.1	18.459	–112.2	10.085
O5(n)–C5(n)–C6(n)–O6(n) <sub>2</sub>	–66.2	11.063	–65.8	10.812	–65.0	11.657	–63.5	4.759
	66.6	15.516	66.1	15.606	67.6	17.933	62.7	–

d: deviation of O4(n) from the least-squares plane defined by the seven O4(n) atoms;  $\tau$ : tilt angle, defined as the angle between the O4(n) plane and the glucose unit planes;  $\phi$  and  $\psi$ : torsion angles around the glycosidic bonds defined as O5(n)–C1(n)–O4(n – 1)–C4(n – 1) and C1(n)–O4(n – 1)–C4(n – 1)–C5(n – 1), respectively;  $\sigma$ : standard deviation of each parameter

<sup>a</sup> Selected geometrical parameter of the X-ray crystallographic structure [42]

<sup>b</sup> Is the absolute value of the deviation of O4(n) from the O4(n) mean plane

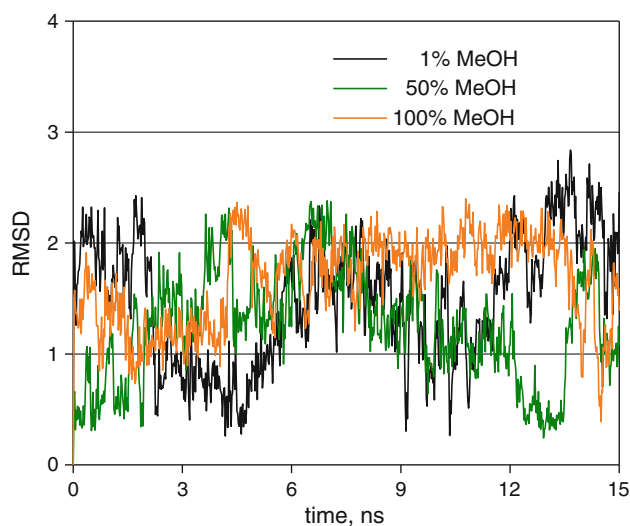


**Fig. 11** Plot of RMSD of  $\beta$ -CD in system of MeOH from the equilibrated structure of  $\beta$ -CD in water, as a function of MD simulation time for all backbone atoms

leave the cavity. The primary hydroxyl group orientation at the C6 rim is in (–) gauche more often than  $\beta$ -CD for 1% concentration. Due to this orientation, the solvent molecules can easily move through the cavity.

In pure ethanol, the occupancy factor for EtOH molecules in the upper part (above O4(n) plane) of cavity is about 0.6. The (–) gauche orientation of C6(n)–O6(n) increases C6 rim diameter. Ethanol molecules can pass through the  $\beta$ -CD cavity easily without blockage by the hydrophilic cluster of water molecules. This has happened in co-solvent systems. All seven intramolecular hydrogen bonds are observed in all periods of simulation.

#### $\beta$ -CD in water/methanol mixtures

A similar picture of the  $\beta$ -CD structural deviation in a water/methanol system from the initial structure, to the deviation found in a water/ethanol system, is observed. The deviation in the water/methanol system is more pronounced than in the ethanol case. The structural information during the simulations obtained from the root mean square deviation (RMSD) from the corresponding initial atomic positions of  $\beta$ -CD, after equilibration for 15 ns, is about 1.26, 1.05, and 0.93  $\text{\AA}$  for  $\beta$ -CD in 1, 50, and 100% methanol, respectively. In methanol solution, the fluctuation of the  $\beta$ -CD structure in dilute solution is also higher than that of  $\beta$ -CD in high concentration solutions, as shown in Fig. 10a and Table 4. The degree of the deviation also depends on the amount of methanol in the system.

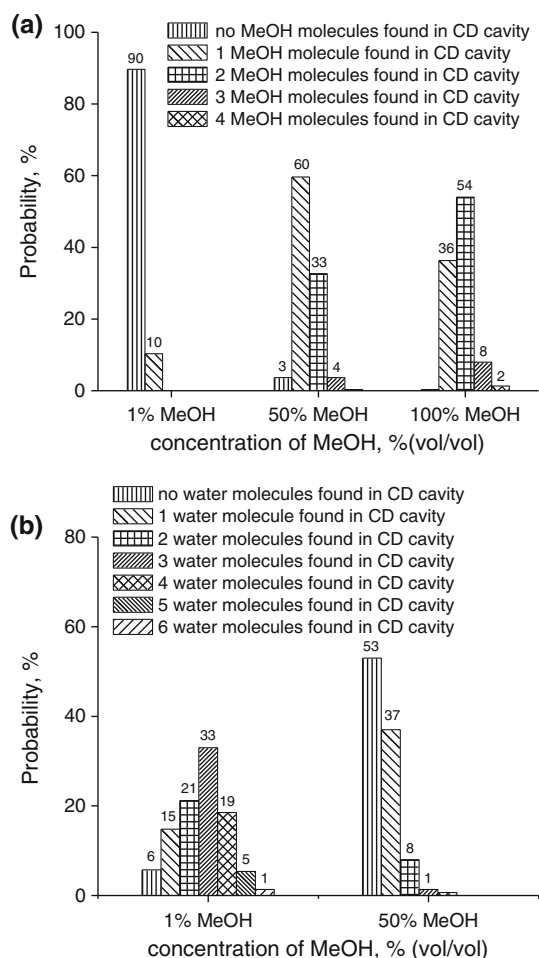


**Fig. 12** Probability distributions of the number of **a** MeOH molecules and **b** water molecules inside  $\beta$ -CD cavity during the MD simulations for 15 ns of  $\beta$ -CD in a MeOH system

The same results as reported in an EtOH system are found. The average structural parameters of  $\beta$ -CD in different concentrations of methanol are not significantly different. However, the degree of the standard deviation,  $\sigma$  depends on the concentration of methanol solution. The standard deviation decreases when the amount of MeOH molecules in solvent increases. The orientations of all seven primary hydroxyl groups (O5(n)–C5(n)–C6(n)–O6(n) torsion angles) are preferred in both (–) and (+) gauche. The (–) orientation is more often observed, with 75, 64 and 62% probability for  $\beta$ -CD in 1, 50 and 100% concentration of MeOH, respectively (see also Fig 10b). The average tilt angle of  $\beta$ -CD in MeOH systems is about 86–88°, which is approximately 9° more than the X-ray crystal structure [42]. The results show the same trend where the simulations give higher tilt angle than that obtained by X-ray in aqueous, EtOH, and MeOH co-solvent systems.

Comparison between the obtained structure with previous  $\beta$ -CD structure in 100% water is done in order to

investigate the change of  $\beta$ -CD structure in the presence of MeOH. RMSD from the equilibrated structure of  $\beta$ -CD in water are about 1.49, 1.26 and 1.67 Å with 1, 50 and 100% MeOH, respectively (Fig. 11). The most interesting point is the orientation of the primary hydroxyl groups. In dilute solution (1% MeOH), C6(n)–O6(n) groups more frequently face out of the cavity than the C6(n)–O6(n) groups of  $\beta$ -CD in aqueous solution. Solvent molecules can easily pass through the cavity without blockage of the primary hydroxyl group at the narrow rim.

The number of encapsulated solvent molecules is reported in Fig. 12. In dilute concentration (1% vol/vol), only one methanol molecule is found inside the cavity with 10% probability. This result supports that methanol does not possess the same degree of hydrophobicity as ethanol. In this concentration, the site most frequently occupied by MeOH molecule is in the upper part (above O4(n) plane) of  $\beta$ -CD cavity (occupancy 0.6).

In higher concentration (50% vol/vol) and pure MeOH, the most frequently occupied site inside the  $\beta$ -CD cavity of the encapsulated methanol molecules is below the O4(n) plane of  $\beta$ -CD with 0.6 and 0.7 occupancy factors for 50 and 100% MeOH, respectively. This most frequently occupied site is in agreement with the X-ray crystallographic structure [42].

## Conclusions

The MD simulations on  $\beta$ -CD in the water/co-solvent systems of ethanol and methanol show asymmetric structures of  $\beta$ -CD during the simulation times of 15 ns. The deviation of the structure of  $\beta$ -CD depends on the type and the concentration of solvent molecules. The structural fluctuation decreases when the concentration of solvent increases. The interaction of  $\beta$ -CD with solvent molecules leads to a distortion of the  $\beta$ -CD rim. When the alcohol molecules are present in the solvent system, the primary hydroxyl groups face out of the cavity. The solvent molecules can easily move through the cavity. For all simulations, the obtained structures have a higher value of the average tilt angle than the structure obtained from X-ray study.

**Acknowledgments** The financial support of the Thailand Research Fund (Grant RSA5080001) and the scholarship from the Office of the Higher Education Commission (Grant 139/2551) are gratefully acknowledged. Moreover, the authors thank Dr. A. Beyer for critical comments.

## References

- Szejtli, J.: Introduction and general overview of cyclodextrin chemistry. *Chem. Rev.* **98**, 1743–1754 (1998)
- Uekama, K., Hirayama, F., Irie, T.: Cyclodextrin drug carrier systems. *Chem. Rev.* **98**, 2045–2076 (1998)

3. Connors, K.A.: The stability of cyclodextrin complexes in solution. *Chem. Rev.* **97**, 1325–1357 (1997)
4. Uekama, K.: Recent aspects of pharmaceutical application of cyclodextrins. *J. Inclusion Phenom. Mol. Recognit. Chem.* **44**, 3–7 (2002)
5. Challa, R., Ahuja, A., Ali, J., Khar, R.K.: Cyclodextrins in drug delivery: an updated review. *AAPS Pharm. Sci. Tech.* **6**, E329–E357 (2005)
6. Takahashi, K.: Organic reactions mediated by cyclodextrins. *Chem. Rev.* **98**, 2013–2034 (1998)
7. Monti, S., Sortino, S.: Photoprocesses of photosensitizing drugs within cyclodextrin cavities. *Chem. Soc. Rev.* **31**, 287–300 (2002)
8. Kano, K., Hasegawa, H.: Interactions with charged cyclodextrins and chiral recognition. *J. Inclusion Phenom. Macrocycl. Chem.* **47**, 41–47 (2001)
9. Harada, A.: Cyclodextrin-based molecular machines. *Acc. Chem. Res.* **34**, 456–464 (2001)
10. Guillaume, Y.C., Guinchard, C.: New statistical approach to a gas chromatography retention model: application to dichlorophenol isomers. *J. Phys. Chem. B* **101**, 8390–8394 (1997)
11. Buschmann, H.J., Knittel, D., Schollmeyer, E.: New textile applications of cyclodextrins. *J. Inclusion Phenom.* **40**, 169–172 (2001)
12. Szenté, L., Szejtli, J.: *Comprehensive supramolecular chemistry*. In: Szejtli, J., Osa, T. (eds.) *Comprehensive Supramolecular Chemistry*, pp. 503–514. Pergamon, Oxford (1996)
13. Tomasella, F.P., Pan, Z., Love, L.J.C.: Effects of selected alcohols on chiral recognition via cyclodextrin inclusion complexation. *J. Supramol. Chem.* **1**, 25–30 (1992)
14. Song, L., Purdy, W.C.: Cyclodextrins and their applications in analytical chemistry. *Chem. Rev.* **92**, 1457–1470 (1992)
15. Loftsson, T., Brewster, M.E.: Pharmaceutical applications of cyclodextrins. 1. Drug solubilization and stabilization. *J. Pharm. Sci.* **85**, 1017–1025 (1996)
16. Pharr, D.Y., Fu, Z.S., Smith, T.K., Hinze, W.L.: Solubilization of cyclodextrins for analytical applications. *Anal. Chem.* **61**, 275–279 (1989)
17. Buvári, A., Barcza, L.: Complex formation of inorganic salts with  $\beta$ -cyclodextrin. *J. Inclusion Phenom. Mol. Recognit. Chem.* **7**, 379–389 (1989)
18. Zukowski, J., Sybilska, D., Jurezak, J.: Resolution of ortho, meta, and para isomers of some disubstituted benzene derivatives via  $\alpha$ - and  $\beta$ -cyclodextrin inclusion complexes, using reversed-phase high-performance liquid chromatography. *Anal. Chem.* **57**, 2215–2219 (1985)
19. Donzé, C., Chatjigakis, A., Coleman, A.W.: Co-solvent modulation of the inclusion selectivity of  $\beta$ -cyclodextrin. *J. Inclusion Phenom. Mol. Recognit. Chem.* **13**, 155–161 (1992)
20. Nelson, G., Patonay, G., Warner, I.M.: Effects of selected alcohols on cyclodextrin inclusion complexes of pyrene using fluorescence lifetime measurements. *Anal. Chem.* **60**, 274–279 (1988)
21. Taghvaei, M., Stewart, G.H.:  $\beta$ -cyclodextrin solubility in reversed-phase high-performance liquid chromatographic eluents. *Anal. Chem.* **63**, 1902–1904 (1991)
22. Chatjigakis, A.K., Donzé, C., Coleman, A.W., Cardot, P.: Solubility behavior of  $\beta$ -cyclodextrin in water/cosolvent mixtures. *Anal. Chem.* **64**, 1632–1634 (1992)
23. Lawtrakul, L., Viernstein, H., Wolschann, P.: Molecular dynamics simulations of [beta]-cyclodextrin in aqueous solution. *Int. J. Pharm.* **256**, 33–41 (2003)
24. Winkler, R.G., Fioravanti, S., Ciccotti, G., Margheritis, C., Villa, M.: Hydration of  $\beta$ -cyclodextrin: a molecular dynamics simulation study. *J. Computer-Aided Mol. Design* **14**, 659–667 (2000)
25. Cai, W., Sun, T., Shao, X., Chipot, C.: Can the anomalous aqueous solubility of  $\beta$ -cyclodextrin be explained by its hydration free energy alone? *PCCP* **10**, 3236–3243 (2008)
26. Raffaini, G., Ganazzoli, F.: Hydration and flexibility of  $\alpha$ -,  $\beta$ -,  $\gamma$ -, and  $\delta$ -cyclodextrin: a molecular dynamics study. *Chem. Phys.* **333**, 128–134 (2007)
27. Lindner, K., Saenger, W.: Crystal and molecular structure of cyclohepta-amylose dodecahydrate. *Carbohydr. Res.* **99**, 103–115 (1982)
28. Frisch, M.J., Trucks, G.W., Schlegel, H.B., Scuseria, G., Scuseria, E., Robb, M.A., Cheeseman, J.R., Montgomery, J.A., Vreven, T., Kudin, K.N., Burant, J.C., Millam, J.M., Iyengar, S.S., Tomasi, J., Barone, V., Mennucci, B., Cossi, M., Scalmani, G., Rega, N., Petersson, G.A., Nakatsuji, H., Hada, M., Ehara, M., Toyota, K., Fukuda, R., Hasegawa, J., Ishida, M., Nakajima, T., Honda, Y., Kitao, O., Nakai, H., Klene, M., Li, X., Knox, J.E., Hratchian, H.P., Cross, J.B., Bakken, V., Adamo, C., Jaramillo, J., Gomperts, R., Stratmann, R.E., Yazyev, O., Austin, A.J., Cammi, R., Pomelli, C., Ochterski, J.W., Ayala, P.Y., Morokuma, K., Voth, G.A., Salvador, P., Dannenberg, J.J., Zakrzewski, V.G., Dapprich, S., Daniels, A.D., Strain, M.C., Farkas, O., Malick, D.K., Rabuck, A.D., Raghavachari, K., Foresman, J.B., Ortiz, J.V., Cui, Q., Baboul, A.G., Clifford, S., Cioslowski, J., Stefanov, B.B., Liu, G., Liashenko, A., Piskorz, P., Komaromi, I., Martin, R.L., Fox, D.J., Keith, T., Al-Laham, M.A., Peng, C.Y., Nanayakkara, A., Challacombe, M., Gill, P.M.W., Johnson, B., Chen, W., Wong, M.W., Gonzalez, C., Pople, J.A.: *Gaussian 03*, Revision C.02 ed. Gaussian, Inc., Wallingford, CT (2004)
29. Bayly, C.I., Cieplak, P., Cornell, W.D., Kollman, P.A.: A well-behaved electrostatic potential based method using charge restraints for deriving atomic charges: the RESP model. *J. Phys. Chem.* **97**, 10269–10280 (1993)
30. Fox, T., Kollman, P.A.: Application of the RESP methodology in the parametrization of organic solvents. *J. Phys. Chem. B* **102**, 8070–8079 (1998)
31. Wang, J., Morin, P., Wang, W., Kollman, P.A.: Use of MM-PBSA in reproducing the binding free energies to HIV-1 RT of TIBO derivatives and predicting the binding mode to HIV-1 RT of efavirenz by docking and MM-PBSA. *J. Am. Chem. Soc.* **123**, 5221–5230 (2001)
32. Case, D.A., Darden, T.A., Cheatham, I.T.E., Simmerling, C.L., Wang, J., Duke, R.E., Luo, R., Merz, K.M., Pearlman, D.A., Crowley, M., Walker, R.C., Zhang, W., Wang, B., Hayik, S., Roitberg, A., Seabra, G., Wong, K.F., Paesani, F., Wu, X., Brozell, S., Tsui, V., Gohlke, H., Yang, L., Tan, C., Mongan, J., Hornak, V., Cui, G., Beroza, P., Mathew, D.H., Schafmeister, C., Ross, W.S., Kollman, P.A.: *AMBER10*. (2006)
33. Duan, Y., Wu, C., Chowdhury, S., Lee, M.C., Xiong, G., Zhang, W., Yang, R., Cieplak, P., Luo, R., Lee, T., Caldwell, J., Wang, J., Kollman, P.: A point-charge force field for molecular mechanics simulations of proteins based on condensed-phase quantum mechanical calculations. *J. Comput. Chem.* **24**, 1999–2012 (2003)
34. Jorgensen, W.L., Chandrasekhar, J., Madura, J.D., Impey, R.W., Klein, M.L.: Comparison of simple potential functions for simulating liquid water. *J. Chem. Phys.* **79**, 926–935 (1983)
35. Ryckaert, J.P., Ciccotti, G., Berendsen, H.J.C.: Numerical integration of the Cartesian equations of motion of a system with constraints: molecular dynamics of n-alkanes. *J. Comput. Phys.* **23**, 327–341 (1977)
36. Snor, W., Liedl, E., Weiss-Greiler, P., Karpfen, A., Viernstein, H., Wolschann, P.: On the structure of anhydrous  $\beta$ -cyclodextrin. *Chem. Phys. Lett.* **441**, 159–162 (2007)
37. Hingerty, B., Klar, B., Hardgrove, G.L., Betzel, C., Saenger, W.: Neutron diffraction of alpha, beta and gamma cyclodextrins: hydrogen bonding patterns. *J. Biomol. Struct. Dyn.* **2**, 249–260 (1984)

38. Betzel, C., Saenger, W., Hingerty, B.E., Brown, G.M.: Circular and flip-flop hydrogen bonding in  $\beta$ -cyclodextrin undecahydrate: a neutron diffraction study. *J. Am. Chem. Soc.* **106**, 7545–7557 (1984)
39. Zabel, V., Saenger, W., Mason, S.A.: Neutron diffraction study of the hydrogen bonding in  $\beta$ -cyclodextrin undecahydrate at 120 K: from dynamic flip-flops to static homodromic chains. *J. Am. Chem. Soc.* **108**, 3664–3673 (1986)
40. Aree, T., Chaichit, N.: A new crystal form of beta-cyclodextrin-ethanol inclusion complex: channel-type structure without long guest molecules. *Carbohydr. Res.* **338**, 1581–1589 (2003)
41. Steiner, T., Mason, S.A., Saenger, W.: Disordered guest and water molecules. Three-center and flip-flop O–H...O hydrogen bonds in crystalline  $\beta$ -cyclodextrin ethanol octahydrate at T = 295 K: a neutron and X-ray diffraction study. *J. Am. Chem. Soc.* **113**, 5676–5687 (1991)
42. Lindner, K., Saenger, W.: Crystal and molecular structures of cyclomaltoheptaose inclusion complexes with HI and with methanol. *Carbohydr. Res.* **107**, 7–16 (1982)